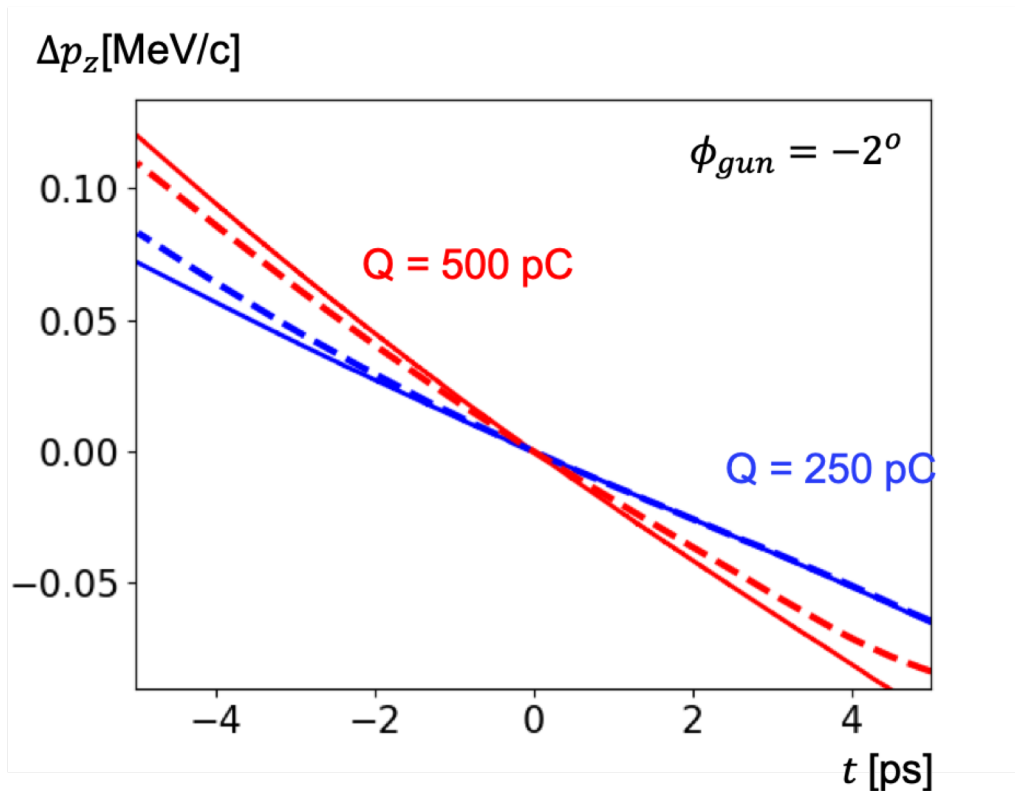


Collective Effects at the Injector Section of the European X-Ray Free-Electron Laser



HELMHOLTZ
RESEARCH FOR GRAND CHALLENGES



Igor Zagorodnov, Frank Brinker,
Ye Chen, Sergey Tomin

S2E Meeting
DESY, Hamburg
September 15, 2020

Outline

- Motivation
- Layout of the injector section and the setup of the measurements
- Measurements and their analysis
- Modelling of the beam dynamics
 - Modelling of the RF gun
 - Wake function of a finite chain of accelerating cavities
 - Particle tracking with collective effects after RF gun
- Comparison between the measurements and the simulations
- Summary

Motivation

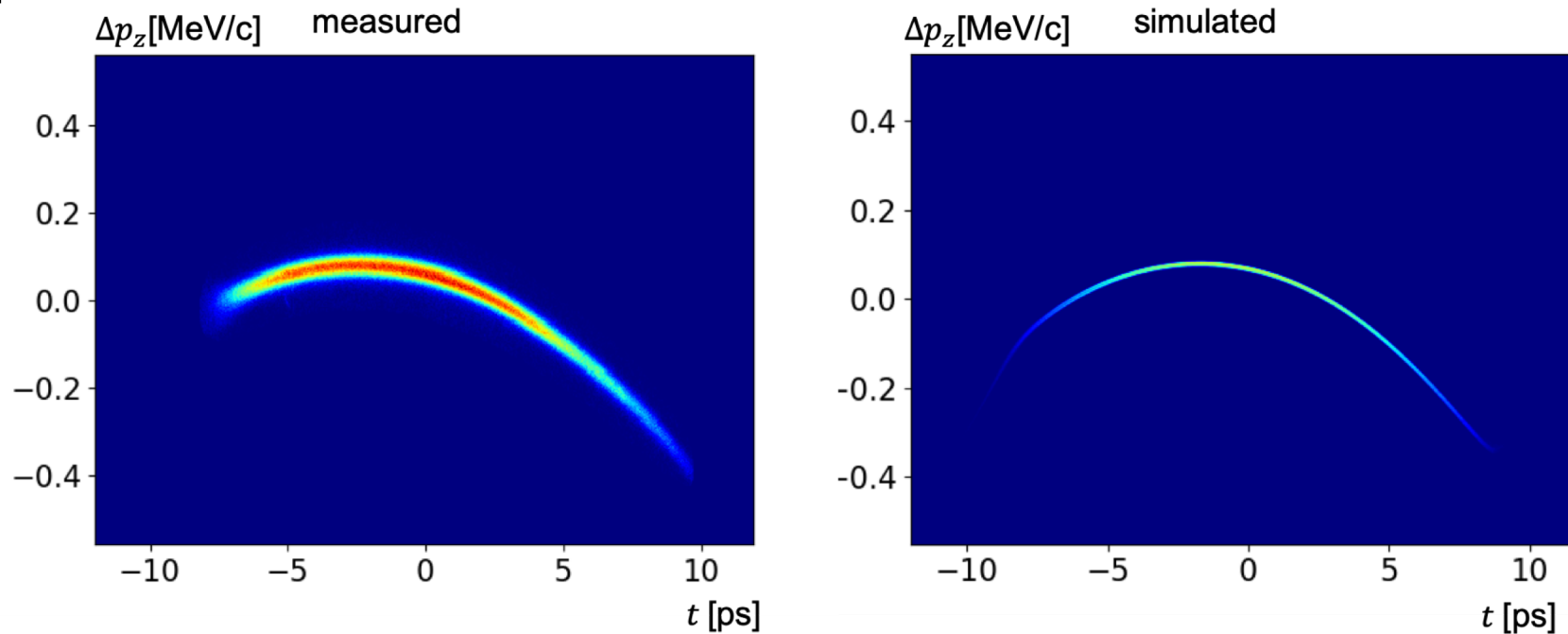
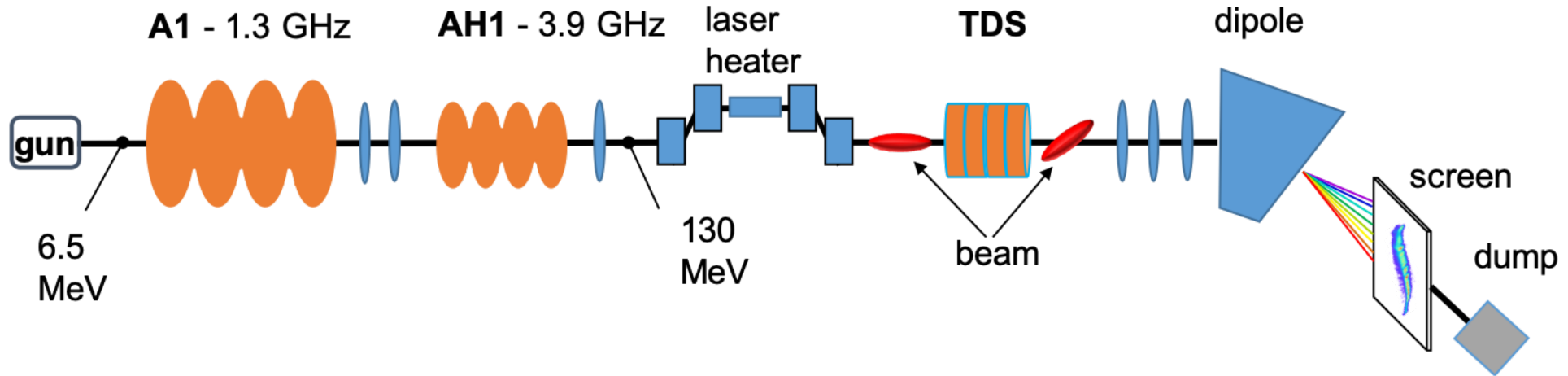
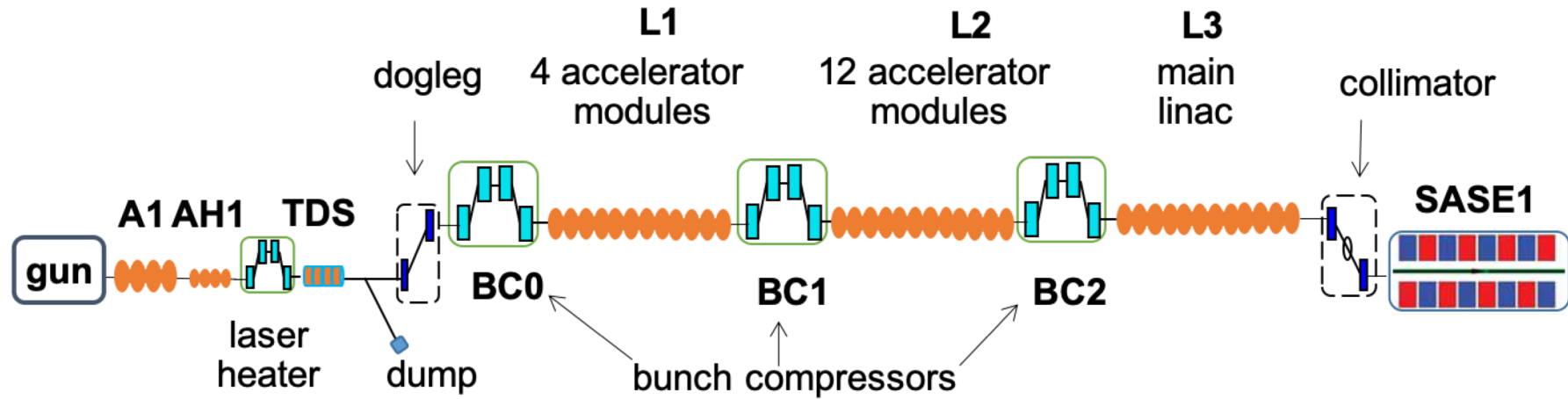


FIG. 3: Comparison of the longitudinal phase space from measurement (left) and from simulation (right) for the bunch charge $Q = 250$ pC , the gun phase $\phi_{gun} = -2^\circ$ and the synchronous phase of cryomodule A1 $\phi_{A1} = 0$.

- The A1 phase of minimal energy spread is usually different from the phase of maximal beam momentum by approximately 1 degree

Layout of the injector section and the setup of the measurements



Measurements and their analysis

The longitudinal component of the electric field on the axis of the gun cavity can be represented as

$$E_z(z, t) = E_z(z) \sin(\omega t + \phi_{MM} + \phi_{gun}), \quad (1)$$

where ϕ_{MM} is the phase of maximal mean momentum of the electron beam, t is a flight time of a reference particle.

At the first step we have done a set of measurements to define a working point of the gun at a bunch charge $Q = 250$ pC. We have found that the gun phase of maximal mean momentum of the electron beam ϕ_{MM} is 44 degrees and the momentum of the beam after the gun is equal to 6.45 MeV/c. As a reference particle we have considered the center of mass of the electron beam.

Measurements and their analysis

The change of the longitudinal momentum in cryomodule A1 can be approximated by expression

$$\Delta p_z(t) = \frac{eV_{A1}}{c} \cos(\omega t + \phi_{A1}), \quad \omega = 2\pi f, \quad (2)$$

where t is the relative time offset to the beam center of mass, e is the electron charge, c is the vacuum light velocity, V_{A1} and ϕ_{A1} are the voltage and the synchronous phase of the cryomodule A1, respectively, and $f = 1.3$ GHz.

The best beam emittance is obtained not in the gun phase of maximal electron beam momentum but at a phase shifted by 2-3 degree. Hence we set the gun phase ϕ_{gun} to -2 degree. Additionally we have done a scan of the gun solenoid strength to find its value for a reasonably small transverse projected emittance of $0.6 \mu\text{m}$.

Measurements and their analysis

At this state of the gun we have done a scan of the phase of cryomodule A1 to define the RF phase of maximal mean momentum of the electron beam. The RF phase of the cryomodule A1 was set to this phase ϕ_{A1}^{RF} . Note that, the exact value of the RF phase is not important for our discussion. We use only the fact that for the RF phase ϕ_{A1}^{RF} (so called "on-crest" phase) the synchronous phase ϕ_{A1} is zero for the bunch charge $Q = 250$ pC and the gun phase $\phi_{gun} = -2^\circ$.

In order to compare the measurement with the simulation and to verify the physical models of different collective effects we need to make not only one measurement but a whole set of scans for different parameters. In the experiment we have done measurements for three different bunch charges (250 pC, 500 pC, 750 pC) and for the gun phases from -8 to 4 degrees. The scan of the gun phase is necessary for two reasons: (1) to define the RF phase ϕ_{MM} of maximal mean momentum and (2) to check that the energy chirp from the gun is correctly reproduced in the simulations.

Measurements and their analysis

$$p_z(t) = \langle \rho(t, p_z) \rangle_{p_z}$$

$$V(\Delta\phi_{A1}) = V(0) / \cos(\Delta\phi_{A1})$$

$$p_z(t, \Delta\phi_{A1}) = p_z^0 + \frac{eV(\Delta\phi_{A1})}{c} \cos(\omega t + \Delta\phi_{A1} + \phi_{A1}^0) + \Delta p_z(t, \Delta\phi_{A1}, p_z^0, \phi_{A1}^0)$$

$$p_z(t, \Delta\phi_{A1})^{(m)} = p_z^{(m)}(\Delta\phi_{A1}) + \langle \rho^{(m)}(t, p_z, \Delta\phi_{A1}) \rangle_{p_z} - \langle \rho^{(m)}(t, p_z, \Delta\phi_{A1}) \rangle_{t, p_z}$$

The last term in the expression (in red) describes the residual mean slice momentum when the RF curvature of cryomodule A1 is subtracted. This term is created by the beam dynamics in the RF gun and by the collective effects after the gun. This term depends only weakly on the RF phase of A1 if the final energy of the beam is kept approximately constant.

Measurements and their analysis

$$(\hat{p}_z^0, \hat{\phi}_{A1}^0) : \min_{p_z^0, \phi_{A1}^0} \left(\left| \langle m(t, p_z^0, \phi_{A1}^0) \rangle_t \right| + \langle \sigma(t, p_z^0, \phi_{A1}^0) \rangle_t \right)$$

$$m(t, p_z^0, \phi_{A1}^0) = \langle \Delta p_z(t, \Delta \phi_{A1}, p_z^0, \phi_{A1}^0) \rangle_{\Delta \phi_{A1}},$$

$$\sigma(t, p_z^0, \phi_{A1}^0) = \langle (\Delta p_z(t, \Delta \phi_{A1}, p_z^0, \phi_{A1}^0) - m(t, p_z^0, \phi_{A1}^0))^2 \rangle_{\Delta \phi_{A1}}^{1/2}$$

$$\Delta p_z(t) = \langle \Delta p_z(t, \Delta \phi_{A1}, \hat{p}_z^0, \hat{\phi}_{A1}^0) \rangle_{\Delta \phi_{A1}}$$

$$\text{for } \Delta \phi_{A1} = -4^\circ, -2^\circ, 0^\circ, 2^\circ, 4^\circ$$

Measurements and their analysis

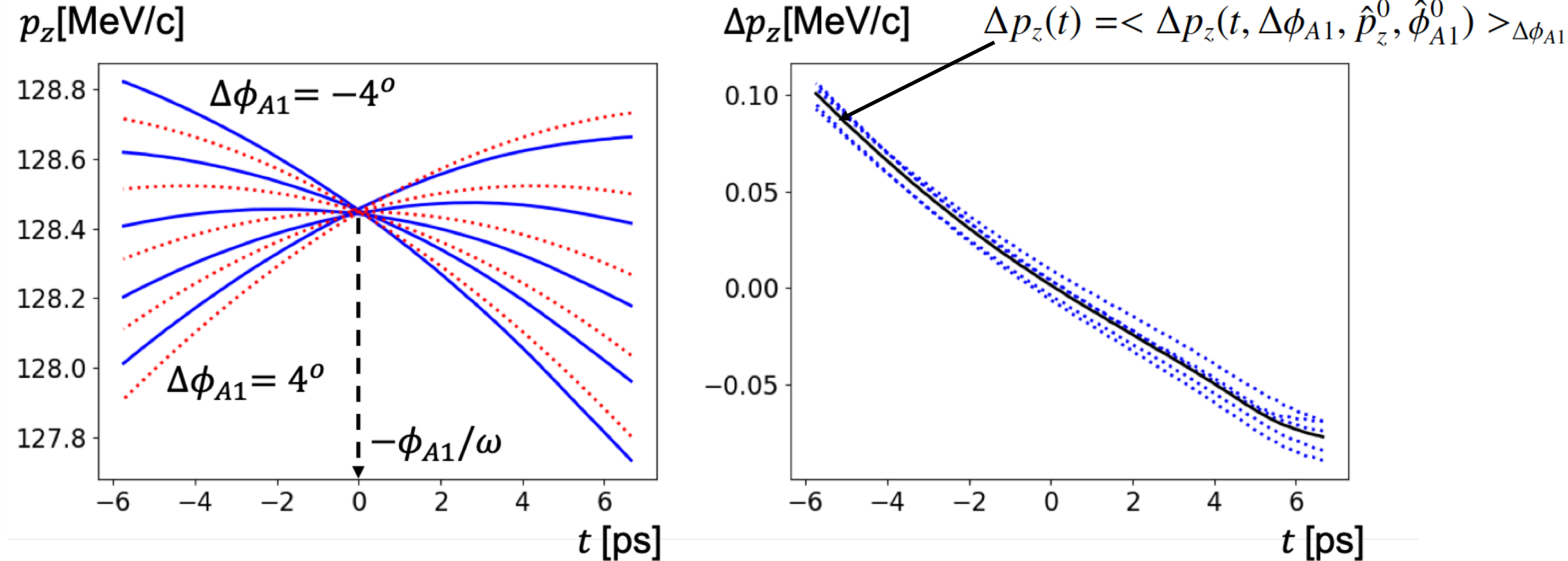


FIG. 4: The left plot presents the measurement of the mean slice momentum for the bunch charge $Q = 250$ pC and the gun phase $\phi_{gun} = -2^\circ$. The right plot shows the residual mean slice momentum after a subtraction of the RF curvature (the dotted red curves in the left plot).

Measurements and their analysis

For the bunch charge $Q = 250$ pC we have found $\hat{p}_z^0 = 5.93$ MeV/c, $\hat{\phi}_{A1}^0 = -0.01^\circ$. The value of \hat{p}_z^0 is different from the measured beam momentum after the gun, 6.45 MeV/c. One of the reasons is the energy loss due to wake fields. From the model of wake fields presented in Section IV B we estimate that the energy loss due to the scattered fields for the bunch charge of 250 pC is equal only to 54 keV. Hence the main sources of this difference are the errors in the energy measurements and the error in the calibration of voltage of cryomodule A1. The value of the synchronous phase $\hat{\phi}_{A1}^0$ is very close to zero as expected.

Measurements and their analysis

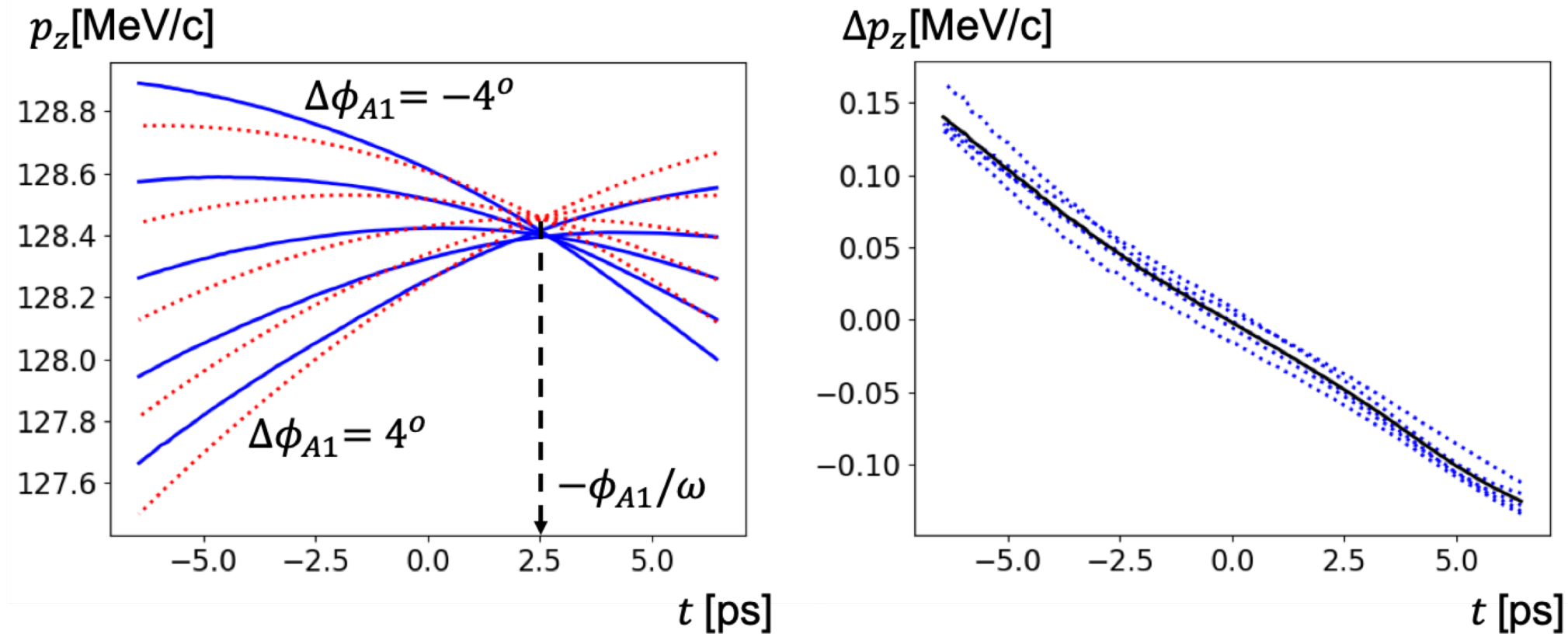


FIG. 5: The left plot presents the measurement of the mean slice momentum (blue solid curves) for the bunch charge $Q = 250$ pC and the gun phase $\phi_{gun} = 4^\circ$. The right plot shows the residual mean slice momentum after a subtraction of the RF curvature (the dotted red curves in the left plot).

Measurements and their analysis

TABLE I: The synchronous phase $\hat{\phi}_{A1}^0$.

	-8°	-5°	-2°	1°	4°
250 pC	1.77	0.82	-0.01	-0.68	-1.19
500 pC	2.17	1.25	0.41	-0.21	-0.71
750 pC	2.38	1.50	0.74	0.21	-0.27

$$\Delta p_z(t) = \frac{eV_{A1}}{c} \cos(\omega t + \phi_{A1}), \quad \omega = 2\pi f,$$

Modelling of the RF gun

The simulations are done with code ASTRA [7]. In the gun simulations we have followed the route used experimentally in setting up the gun. The scan of the RF gun phase for the bunch charge of 250 pC resulted in the maximal mean momentum phase (ϕ_{MM}) of 43° , which agrees reasonably with the phase defined in the experiment. The strength of the solenoid field was chosen the same way as in the experiment to produce a transverse emittance of $0.6 \mu\text{m}$ after cryomodule A1.

In our simulations we use 4×10^5 macro-particles. As for calculating the slice parameters we have used 5×10^3 particles per slice. These calculations are done accordingly for the same set of bunch charges as in the experiment: 250 pC, 500 pC and 750 pC. For each charge set point, the phase ϕ_{MM} (see Eq. (1)) is set as 43° and 5 different gun phases ϕ_{gun} are considered: $-8^\circ, -5^\circ, -2^\circ, 1^\circ, 4^\circ$. The electron bunches are tracked through the RF gun in presence of space charge forces till the entrance of cryomodule A1. The obtained particle distributions are then used for further particle tracking as well as the analysis as described in the next sections.

TABLE II: Injector parameters.

subsection	parameter	
laser	rms length, ps	2.7
	width, mm	1-1.5
RF cavity	frequency, GHz	1.3
	maximal field on cathode, MV/m	56.3
	phase, degree	35-47
solenoid	Magnetic field, T	0.216

Wake function of a finite chain of accelerating cavities

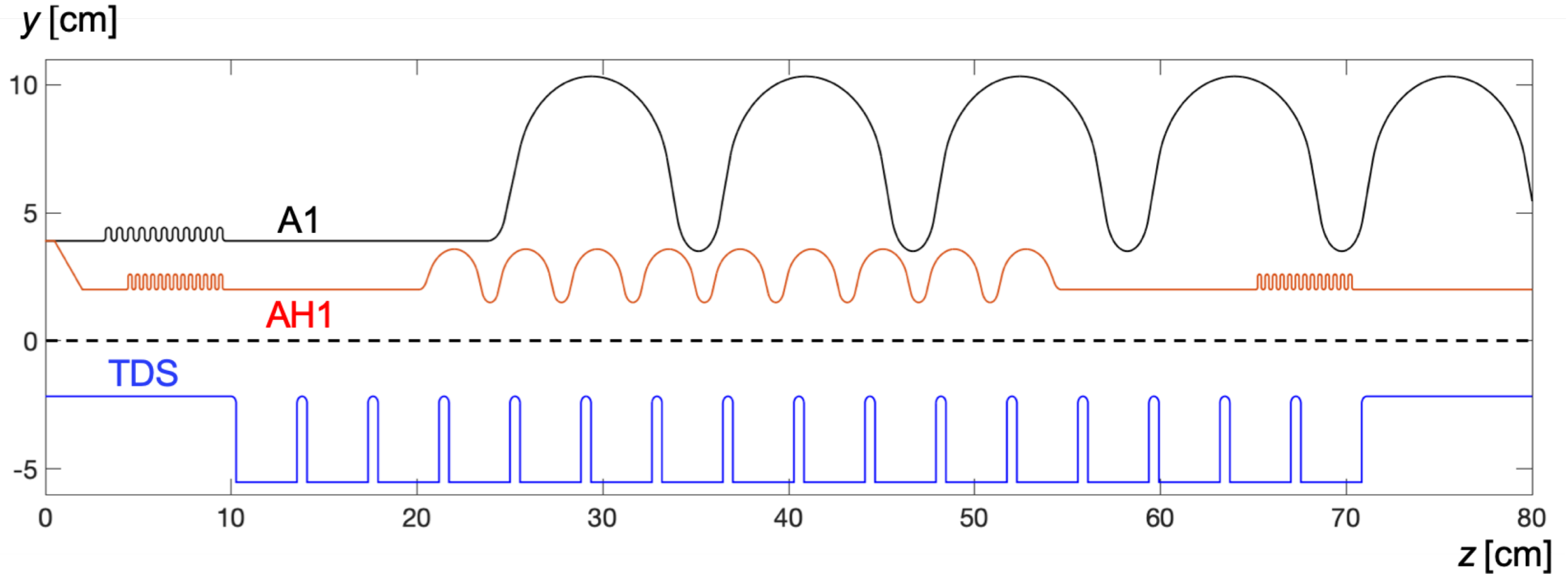


FIG. 6: The geometry of RF modules installed in the injector section of the European XFEL.

Wake function of a finite chain of accelerating cavities

$$w_z(\mathbf{r}, s) = w_z(s) + w'_\perp(s)(x_0x + y_0y) + O(\Delta r^3),$$

$$w_z(s) \equiv w_z(\mathbf{0}, s), \quad w'_\perp(s) \equiv \frac{\partial^2 w_z}{\partial x \partial x_0}(\mathbf{0}, s),$$

$$w_\perp(\mathbf{r}, s) = w_\perp(s)(x_0\mathbf{e}_x + y_0\mathbf{e}_y) + O(\Delta r^2),$$

$$w_\perp(s) = \int_{-\infty}^s w'_\perp(s') ds'.$$

Wake function of a finite chain of accelerating cavities

$$w_z(s) = \theta(s) \left(A e^{-\sqrt{k_0 s}} + B \frac{\cos((k_1 s)^\alpha)}{\sqrt{s + k_2 s}} + C \cos(k_3 s) + D \delta(s) \right),$$

$$W_{z,i}(s) = \int_{-\infty}^s w_z(s - s') \lambda_{\sigma_i}(s') ds',$$

$$\delta_z = \sum_i \|\hat{W}_{z,i} - W_{z,i}\|$$

TABLE III: The coefficients of the function $w_z(s)$.

	A	k_0	B	k_1	α	k_2	C	k_3	D
	V/pC	1/mm	V/pC	1/mm		1/mm	V/pC	1/mm	V/pC
A1	287	0.413	4.75	35.0	0.746	1.52	12.1	0.181	0
AH1	711	1.94	1.50	106	0.661	0.201	49.2	0.154	0.0114
TDS	40.7	0.239	0.524	6.54	0.655	0.140	1.57	0.159	0

$\lambda_{\sigma_i}, \sigma_i = 10, 15, 25, 50, 250, 500, 100, 2000 \mu\text{m}.$

Wake function of a finite chain of accelerating cavities

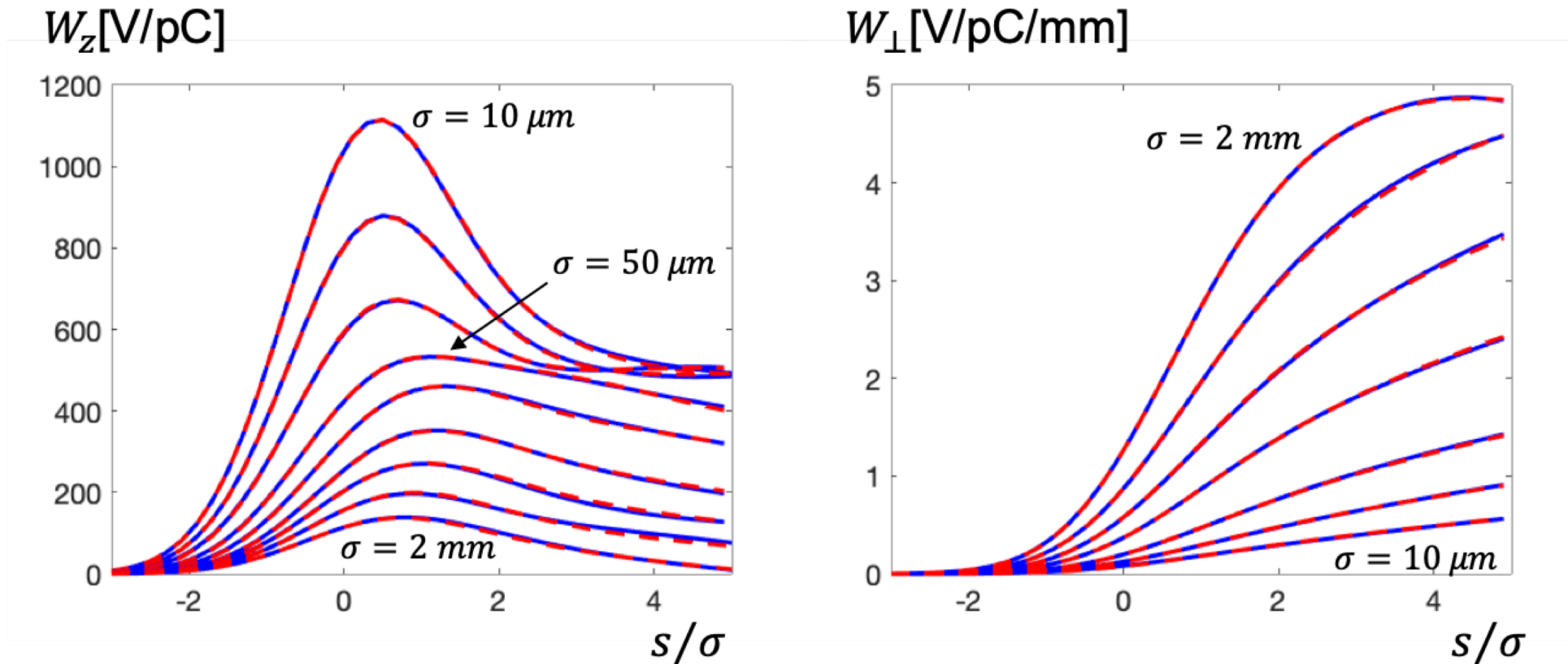


FIG. 7: The longitudinal and the transverse wake potentials of the Gaussian bunches in the high harmonic cryomodule AH1. The bunch length is varied between $10 \mu m$ and $2 mm$. The numerical results from code ECHO are shown by solid blue curves. The analytical approximations are shown by dashed red curves.

Wake function of a finite chain of accelerating cavities

$$w_{\perp}(s) = \theta(s) \left(A' \left(1 - (1 + \sqrt{k'_0 s}) e^{-\sqrt{k'_0 s}} \right) + B' \frac{\sqrt{s}}{1 - \frac{1}{b' s}} + C' \sin(k'_2 s) \right).$$

TABLE IV: The coefficients of the function $w_{\perp}(s)$.

	A'	k'_0	B'	k'_1	C'	k'_2
	V/pC/mm	1/mm	V/pC/mm	1/mm	V/pC/mm	1/mm
A1	1.03	0.426	3.63	0.0664	0.113	0.232
AH1	2.75	2.47	22.9	0.00968	0.645	0.287
TDS	0.0863	0.714	3.81	0.0135	0.0675	0.181

K. Bane, M. Sands, Wakefields of very short bunches in an accelerating cavity, Report No. SLAC-PUB-4441, SLAC, 1987.

Bane K.L.F., Short-range dipole wakefields in accelerating structures for the NLC, Report No. SLAC-PUB-9663, SLAC, 2003.

I. Zagorodnov, T. Weiland, M. Dohlus, Wake fields generated by the LOLA-IV structure and the 3rd harmonic section in TTF-II, Report No. TESLA 2004-01, DESY, 2004.

Wake function of a finite chain of accelerating cavities

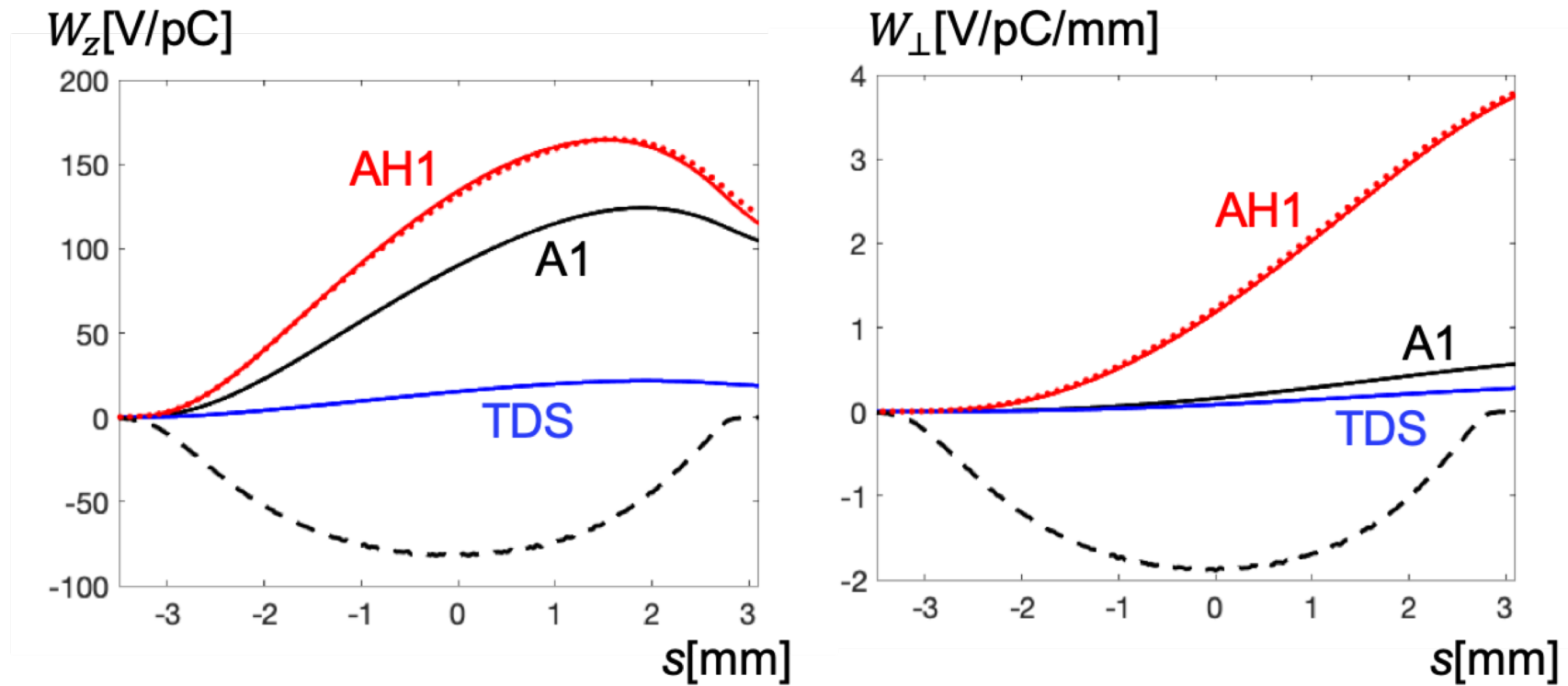
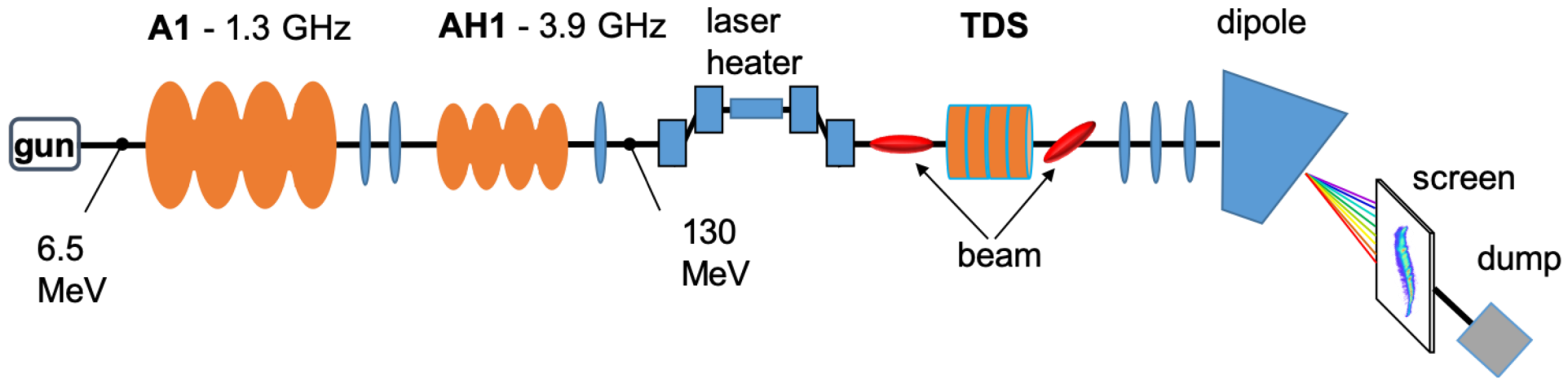


FIG. 8: The longitudinal and the transverse wake potentials of the bunch with the bunch charge 500 pC at the gun phase of -2° . The dashed line shows the bunch shape in arbitrary units. The solid curves present the wake potentials obtained from the analytical representations. The dots present the wakes for AH1 obtained by direct numerical solution of the Maxwell's equations in ECHO.

Wake function of a finite chain of accelerating cavities



■ Ocelot

- external RF fields analytically
- self-fields with 3D Poisson equation
- CSR fields with 1D projected model
- particle motion with transport matrices of second order
- chamber with wakes

Comparison between measurements and simulations

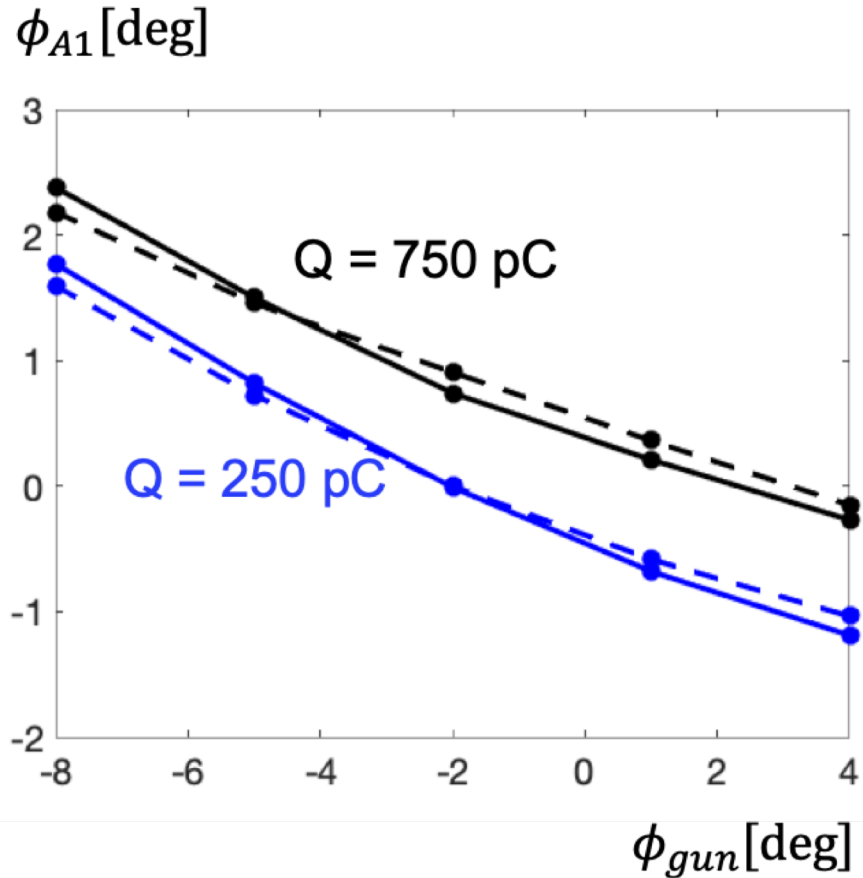


TABLE I: The synchronous phase $\hat{\phi}_{A1}^0$.

	-8°	-5°	-2°	1°	4°
250 pC	1.77	0.82	-0.01	-0.68	-1.19
500 pC	2.17	1.25	0.41	-0.21	-0.71
750 pC	2.38	1.50	0.74	0.21	-0.27

FIG. 9: Evolution of the synchronous phase $\hat{\phi}_{A1}^0$ of cryomodule A1 due to change of the gun phase ϕ_{gun} . The dashed curves present the measured data. The results of the simulations are shown by solid lines.

Comparison between measurements and simulations

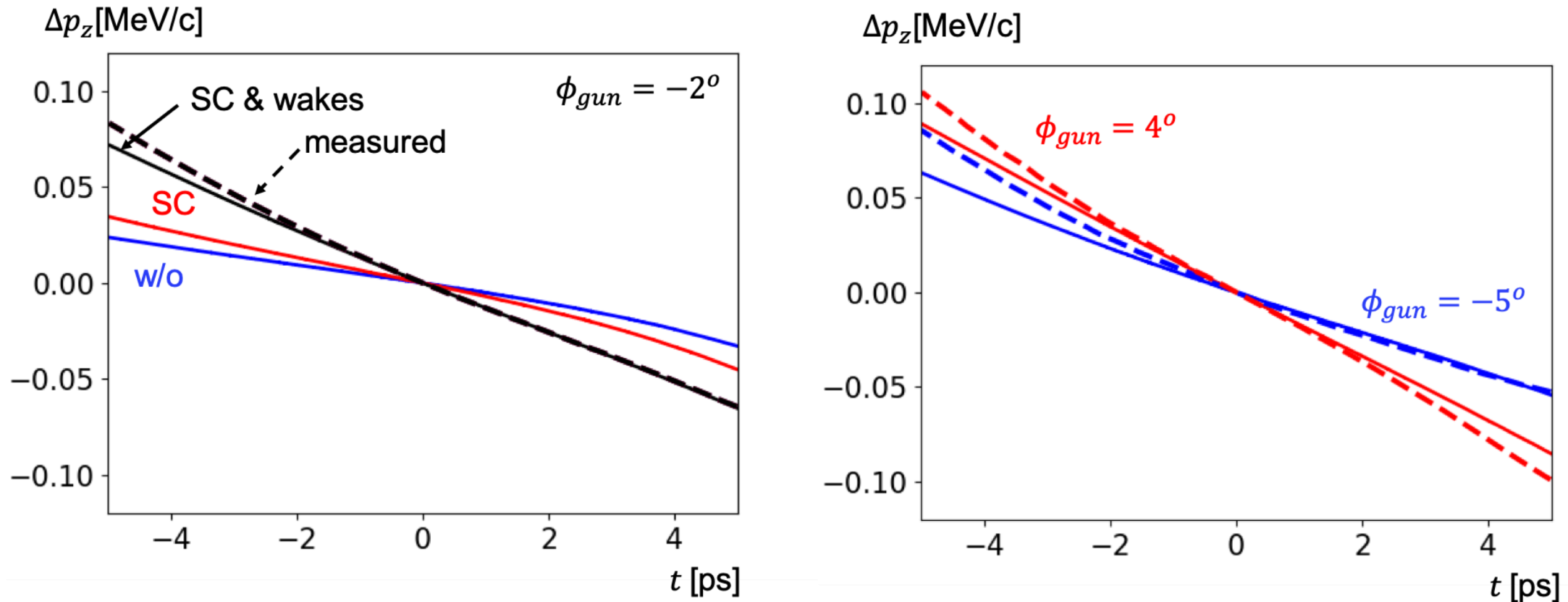


FIG. 10: Comparison of the measurements with simulations for the bunch charge $Q = 250$ pC. The dashed lines represent the measurement data. The solid lines show the results obtained from the simulations.

Comparison between measurements and simulations

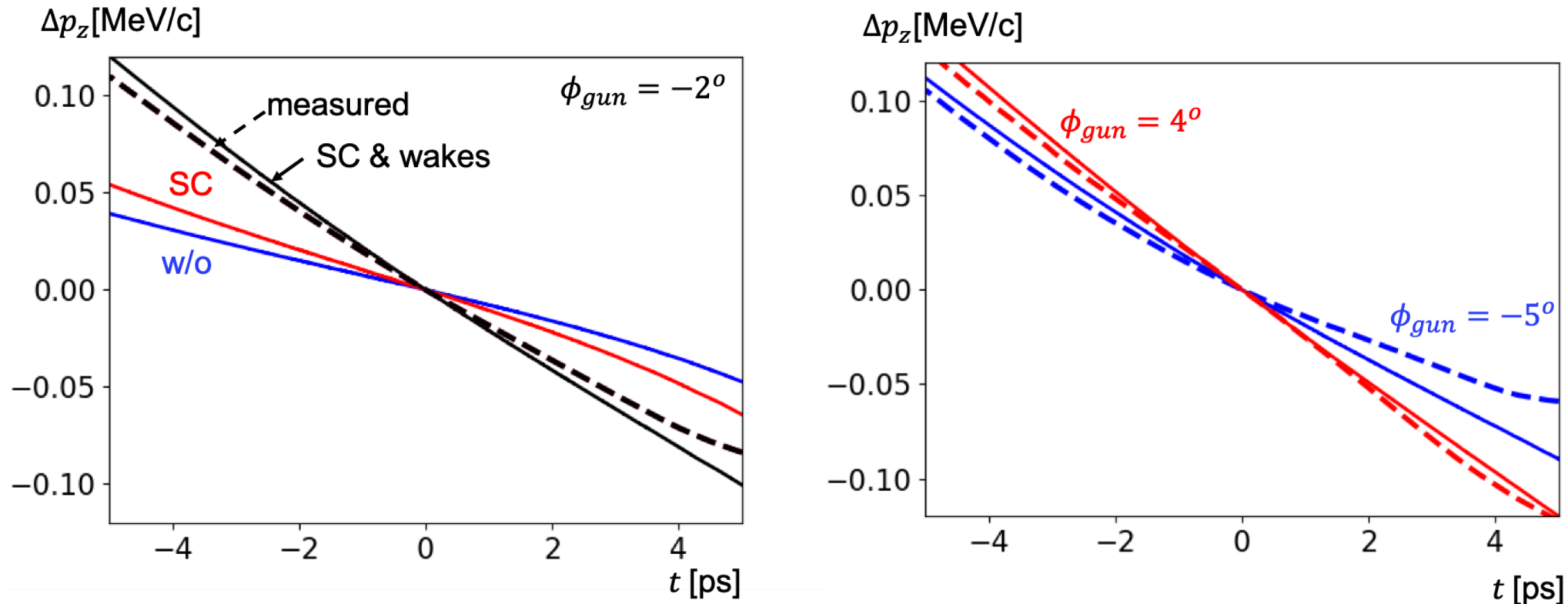


FIG. 11: Comparison of the measurements with simulations for the bunch charge $Q = 500$ pC. The dashed lines represent the experimental results. The solid lines show the results of the simulations.

Comparison between measurements and simulations

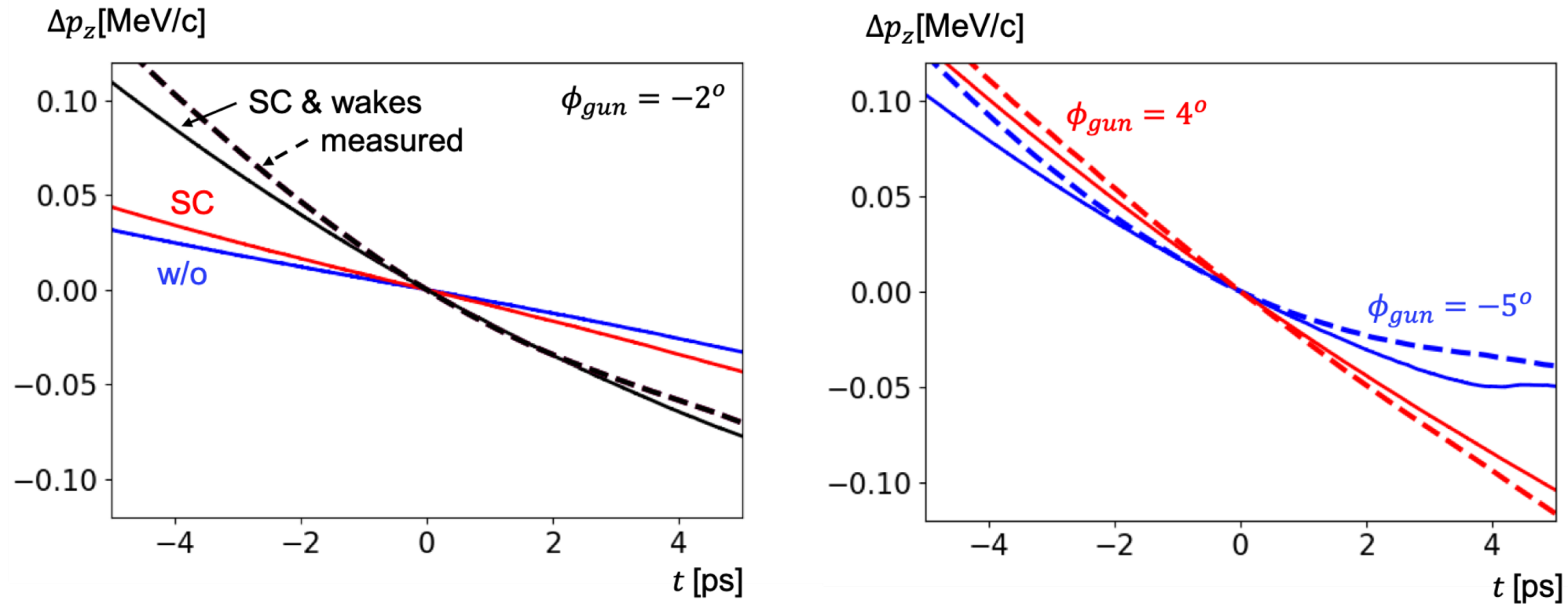


FIG. 12: Comparison of the measurements with simulations for the bunch charge $Q = 750$ pC. The dashed lines represent the measurement data. The solid lines show the simulation results.

Comparison between measurements and simulations

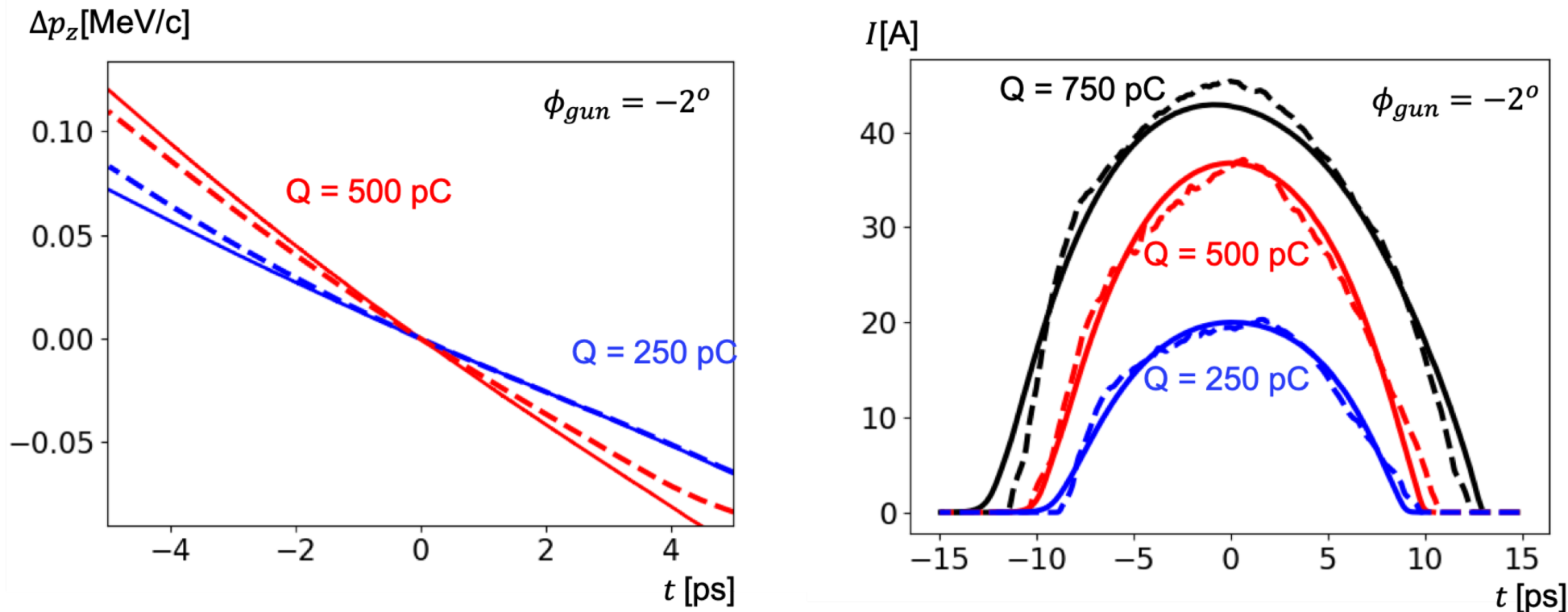


FIG. 13: The left plot compare the residual mean slice momentum for different bunch charges at the gun phase $\phi_{gun} = -2^\circ$. The right plot compares the current profiles for different bunch charges at the same gun phase. The dashed lines present the results of the measurements. The solid lines show the simulation results.

Summary

- We have suggested a method for accurately identifying the synchronous phase of the RF module
- It allows to extract the correlation in the mean slice momentum due to the RF fields and simplifies the comparison between measurement and simulation
- A new model of the wake function in the finite chain of RF cavities is suggested and cross-checked with the simulations as well as the measurements
- The time-resolved measurements of mean slice momentum along the electron bunch proves the theoretical model of collective effects not only quantitatively but also qualitatively.

Acknowledgments

The authors thank W. Decking, M. Dohlus and M. Krasilnikov for helpful discussions. We thank members of the European XFEL team for providing help and conditions to carry out the measurements.